Received June 10, 2020, accepted June 21, 2020, date of publication June 25, 2020, date of current version July 7, 2020.

Digital Object Identifier 10.1109/ACCESS.2020.3004895

A Dual Circularly Polarized Patch Antenna With High Isolation for MIMO WLAN Applications

ENZE ZHANG[1], ANDREA MICHEL[2], (Member, IEEE), MARCOS RODRIGUEZ PINO[3], PAOLO NEPA[2], (Senior Member, IEEE), AND JINGHUI QIU[1]

[1]Department of Electronics and Information Engineering, Harbin Institute of Technology, Harbin 150001, China
[2]Department of Information Engineering, University of Pisa, 56122 Pisa, Italy
[3]Department of Electrical Engineering, University of Oviedo, 33203 Gijón, Spain

Corresponding author: Enze Zhang (zez1992@foxmail.com)

This work was supported in part by the National Natural Science Foundation of China under Grant 61731007, Grant U1633202 and in part under project GRUPIN-IDI/2018/000191.

ABSTRACT A dual circularly polarized (CP) stacked patch antenna for Multiple-Input Multiple-Output (MIMO) WLAN applications (2.4-2.485 GHz) is presented, which exploits a square ring slot feeding technique. The antenna occupies an overall area of 96 mm × 96 mm × 39 mm, when also including the metal reflector. The 7-dBic gain antenna prototype presents an axial ratio lower than 2.5 dB as well as a port isolation higher than 25 dB. An envelope correlation coefficient (ECC) lower than 0.02 is also achieved among the two ports, thanks to the polarization orthogonality. Moreover, the stacked patch has been duplicated and used in a two-antenna system for a 4 × 4 MIMO WLAN which fits an overall volume of 157 mm × 96 mm × 39 mm. Antenna performance in terms of S-Parameters, gain, axial ratio, ECC and channel capacity are compared and discussed, together with the effect of the inter-element distance.

INDEX TERMS Circular polarization, dual-CP, isolation, patch antenna, WLAN, multiple-input multiple-output, MIMO, diversity, square ring slot, stacked patch.

I. INTRODUCTION

Multiple-Input Multiple-Output (MIMO) technology has caught significant attention because of its high data rate, good reliability and spectral efficiency, for assigned bandwidth and power level, to overcome multipath fading in rich scattering environment [1]–[3].

Among others, WLAN MIMO systems are of interest for the scientific community and they are deployed to improve wireless communication among electronic devices (e.g. computers, laptop, smartphones) [4]. WLAN systems use access points or base stations to provide connectivity for the wireless device [5]. Typically, the radiating elements (2 or 4 into the same device) are linearly polarized (LP) and orthogonally placed to allow for satisfactory field uncorrelation [6]–[9]. However, the possibility of using circularly polarized (CP) radiators has also been considered [10]. Compared with LP antennas, CP antennas are good at overcoming the multipath interferences as well as polarization mismatch. More in detail, an analysis of the MIMO performance attainable by employing orthogonally-polarized CP radiators has proved that CP radiators are capable of obtaining greater eigenvalues, as a function of the MIMO antenna orientation, than orthogonally polarized LP radiators [10].

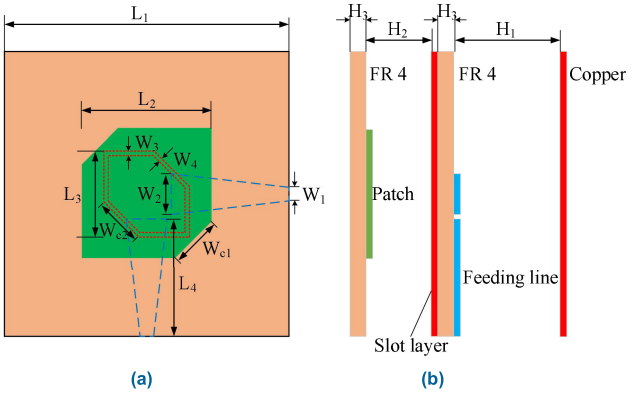

FIGURE 1. (a) Top view; (b) stack-up of the patch fed through a square-ring slot.

In this context, ground radiation CP antennas have been proposed for MIMO WLAN applications [11]. There, the two antennas share the same ground plane, and thanks to a tunable metal strip they are able to generate two

The associate editor coordinating the review of this manuscript and approving it for publication was Luyu Zhao.

orthogonal CP fields, thus allowing for an isolation level higher than 20 dB, and an Envelope Correlation Coefficient (ECC) lower than 0.1. Dual-polarized triple-band MIMO antenna for WLAN and WiMAX applications was proposed in [12]. At the WLAN band, the two radiating elements generate LP fields, but at the WiMAX band (frequency range 3.31-3.84 GHz) the proposed layout is able to radiate two orthogonal CP fields while guaranteeing an isolation higher than 18dB and an ECC lower than 0.02. In [13], two dual-band polygon shaped CPW-fed monopole antennas were designed for a CP MIMO WLAN system. Furthermore, in [14], a two-port omnidirectional CP dielectric resonator antenna (DRA) with polarization diversity was proposed. Each cylindrical DRA (diameter of 49.5 mm) is made of a dielectric material with $\varepsilon_r = 10$, and it is fed by a hybrid coupler printed on a FR-4 substrate below the dielectric cylinder. As a result, an axial ratio lower than 3 dB and an isolation higher than 15 dB are obtained at each port, as well as an ECC lower than -25 dB. CP dielectric resonator antennas are also proposed in [15] for WLAN applications at 5 GHz. In [16], a broadband 94 mm $\times$ 94 mm $\times$ 1.6 mm CP two-element planar inverted-F antenna (PIFA) with pattern diversity and high isolation is shown, for multimode global navigation satellite systems (GPS/GLONASS/Galileo/Compass). Axial ratio assumes values lower than 3dB in the entire frequency band, while the mutual coupling and the ECC are lower than -14dB and 0.02, respectively. Moreover, an array of 8 CP microstrip antennas was proposed in [17] for IEEE 802.11ac MIMO WLAN system. It is worth mentioning that two-ports CP antennas with high isolation at the S-band are recently investigated for simultaneously transmit and receive systems (STARS). However, in that case higher isolation levels (even higher than 100 dB) are obtained by means of ad-hoc feeding lines which are connected to multiple radiating elements [18]. Thus, their multiple antenna elements and feeding network require for a volume which is much larger than that available in commercial WLAN routers or access points.

In this paper, a two-port dual CP stacked patch antenna is designed to be used in a 4 $\times$ 4 MIMO WLAN system. Specifically, the 96 mm $\times$ 96 mm $\times$ 39 mm (0.78 $\lambda\times$ 0.78 $\lambda\times$ 0.32 λ) single radiating element here discussed consists in a stacked chamfered patch electromagnetically fed by a ring slot. The novel contribution of the proposed antenna can be summarized as follows.

- As discussed in [10], a CP MIMO system is suitable to achieve better performance in terms of diversity gain and channel capacity, when compared to LP MIMO systems, when antennas are not perfectly aligned. Here, to reduce the occupied area, a dual-port dual-circularly polarized aperture-shared radiating element is optimized, while guaranteeing a relatively high isolation level between the two ports. To take advantage of the polarization diversity, two orthogonal circularly polarized fields are radiated from two different ports, thus allowing for low ECC values and good MIMO performance in terms of multiplexing efficiency and channel capacity. Then, a second radiating element has been added to exploit a spatial diversity gain and improve the 4 $\times$ 4 WLAN MIMO system performance, while keeping a relatively compact size.
- Differently from other solutions, high isolation is obtained without the need of specific matching or decoupling networks. This is mainly due to the adopted ring slot feeding technique [19]–[22]. With respect to other slot-coupling feeding techniques for dual-polarized patch antennas, the considered feeding technique exhibits a simpler structure and a valuable symmetry property with respect to the two feeding ports, so guaranteeing a natural higher isolation.
- CP ring slot antennas for WLAN and WiMAX applications have been proposed in the literature [21], [22]; in this paper, a dual-port dual-circularly polarized antenna is obtained without implementing any

sequential rotation feeding technique which requires more space.

The detailed design of the proposed antenna is discussed in Section II, also highlighting the effect of some key parameters. Numerical and experimental results are shown and discussed in Section III. A 4 $\times$ 4 MIMO WLAN antenna system is analyzed in Section IV, evaluating the performance in terms of ECC and channel capacity. Conclusions are drawn in Section V.

II. DUAL-CP ANTENNA LAYOUT

Fig. 1 shows the layout of the slot-coupled patch antenna, which consists of two FR4 laminates of thickness 1.53 mm ($\varepsilon_r = 4.3$, $\tan\delta = 0.025$) separated by an air gap of height $H_2 = 12.61$ mm. The microstrip feed lines are printed on the bottom side of the lower laminate, while the ring slot is etched on the top of the same laminate.

Aperture coupling feed was first proposed by Pozar in 1985 [24] and includes several advantages, like shielding of the antenna from feeding-network spurious radiation and antenna bandwidth enlargement. Typically, rectangular slots excited by microstrip lines are used to electromagnetically feed a printed patch antenna. Coupling of the slot to the dominant mode of the patch and the microstrip line occurs because the slot interrupts the longitudinal current flow [25]. Recently, a ring slot was proposed to electromagnetically feed the microstrip patch antenna [19]–[22]. In particular, in [19] and [20] two-ports linearly polarized patch antennas excited by a square ring slot were proposed for WiMAX applications (3.3-3.8 GHz). Four dual-port linearly polarized aperture-coupled antennas are then combined together in [21] with a sequential rotation feeding technique, to achieve a high polarization purity CP radiated field. It is worth noting that the presence of the matching and delay network limits the compactness of the overall structure, and it may represent a disadvantage for some applications. Furthermore, in [22] a single-feed circularly polarized aperture-coupled square ring slot microstrip antenna was proposed. There, circular polarization is achieved with only one port by introducing a

TABLE 1. Structure parameters.

Parameter	Value (mm)	Parameter	Value (mm)
L_1	96.00	W_1	1.80
L_2	39.50	W_2	11.70
L_3	27.40	W_3	1.18
L_4	38.60	W_4	0.97
H_1	21.90	W_{c1}	16.20
H_2	14.20	W_{c2}	17.50
H_3	1.53		

slight asymmetry in both the square ring and patch geometries. The here described antenna solution consists of a dual-port dual-circularly polarized aperture-coupled microstrip patch excited by a ring slot. Differently from [22], two orthogonal circular polarized fields can be radiated by the same aperture-shared dual-port radiating element without adopting a bulky matching and phase-delay networks.

As in ring slot-coupling feeding techniques, the perimeter of the initial $L_3 \times L_3$ square ring slot was set close to the wavelength at the resonating frequency. Two orthogonal microstrip feeding lines were used to feed the slot at two consecutive edges. A printed $L_2 \times L_2$ square patch was then placed at a distance H_2. Its side is slightly different from $\lambda/2$ to obtain a slightly different resonant frequency [24]. The distance H_2 was parametrically optimized together with the upper patch size to get a resonance at the WLAN band.

Hence, an asymmetry has been introduced in both the ring slot and patch geometries to generate a circularly polarization at both the ports [22]. Several different perturbations have been proposed in the literature to excite the two orthogonal fundamental modes of a patch antenna. In this respect, it is worth mentioning the diagonal fed nearly square patch, the corner-truncated patch and the square patch with peripheral cuts or with tuning stub [22], [23]. In this solution, two opposite corners of both the ring slot and resonant patch have been chamfered to obtain a corner-truncated configuration.

Finally, a metallic reflector is placed at a distance H_1 from the bottom of the lower substrate to limit the back-radiation and increase the broadside gain. Since the layout is symmetric with respect to the two input ports, identical radiation and input impedance properties are expected for the two ports. A set of geometrical parameters listed in Table 1 has been optimized to satisfy return loss and port isolation requirements in the WLAN working band (2.4 – 2.485 GHz). The ring slot, with side length $L_3 = 27.4$ mm and chamfering length $W_{c2} = 17.5$ mm, is etched on the top side of the lower substrate. The 39.5 mm × 39.5 mm ($L_2 \times L_2$) patch with chamfering length $W_{c1} = 16.2$ mm is printed on the bottom side of the upper FR4 laminate. The distance H_1 between the lower laminate and the reflector is set at 21.9 mm.

By using a tapered-width stub, a wider impedance bandwidth can be achieved. As shown in Fig. 2, as the stub terminal width W_2 increases, the reflection coefficient improves from −8 to −12 dB.

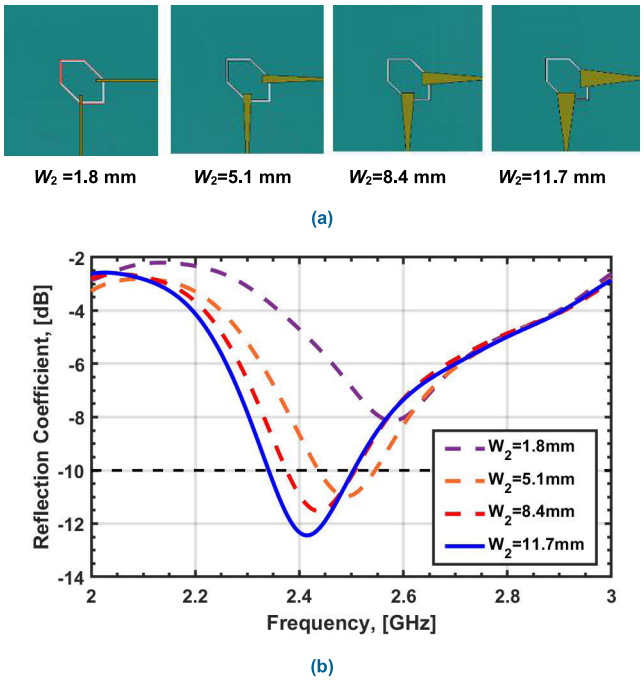

FIGURE 2. (a) Steps used in designing the proposed antenna feeding line; (b) simulated S_{11} for the different stub terminal width W_2.

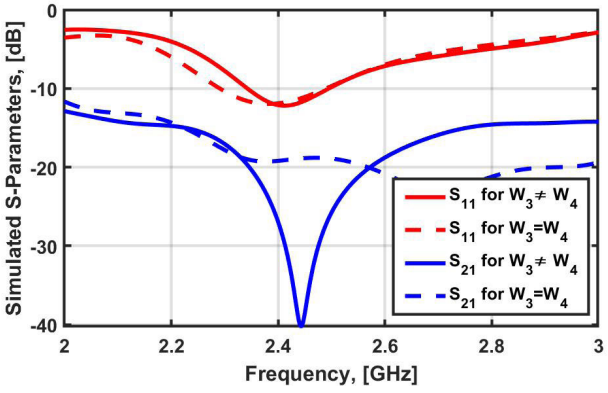

FIGURE 3. Comparison of whether import different width slot structure in terms of S-parameters.

As shown in Fig. 1(a) a non-uniform-width slot structure (W_3 and W_4) has been adopted in order to enhance the isolation performance. Compared to the structure of a uniform width slot W_3, a higher isolation between the two ports is achieved when W_3 and W_4 are different, as shown in Fig. 3 where the two configurations are compared in terms of reflection coefficient and isolation. The port isolation increases from 18 dB to 27 dB in the WLAN working band, while the impedance matching remains almost stable. This is also confirmed by the electric field distribution shown in Fig. 4, where a minimum of electric field is obtained in the slot in correspondence of the second port feed line. Indeed, a stationary field distribution is obtained in the square ring slot [19]–[22]. The final dimensions selected for the designed antenna are shown in Table 1.

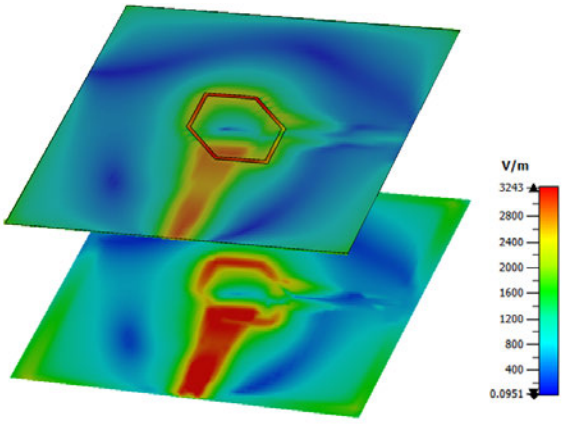

FIGURE 4. E-field distribution with different slot width, W_3 and W_4, at 2.45 GHz, when *Port* 1 is fed and *Port* 2 is impedance matched. Top plot with E-field distribution at slot layer. Bottom plot with E-field distribution at the feeding line layer.

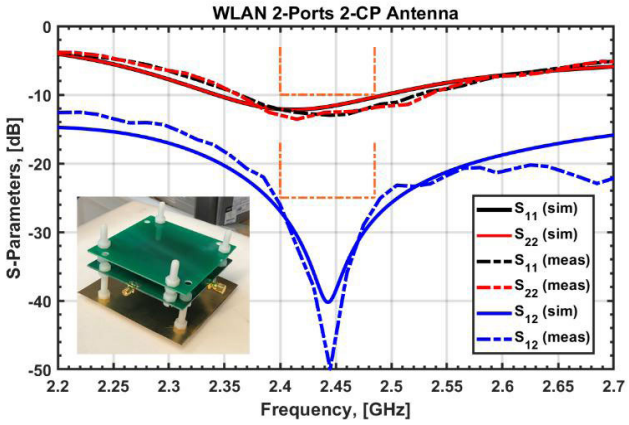

FIGURE 5. Simulated and measured S-parameters of the antenna.

III. NUMERICAL AND EXPERIMENTAL RESULTS

An antenna prototype has been fabricated for validation, and it is shown in the inset of Fig. 5. The simulated and measured S-parameters are also shown in Fig. 5, demonstrating a good agreement. The measured −10 dB bandwidth is found to be in the range 2.36 - 2.53 GHz (7%), for both ports due to the symmetric structure. An isolation of 25 dB is obtained from 2.39 to 2.49 GHz.

In Fig. 6, the proposed antenna is shown in the anechoic chamber during radiation pattern measurements, at the measurement facilities of the University of Oviedo. The simulated and measured LHCP and RHCP radiation patterns in XZ and YZ planes, at 2.44 GHz, are shown in Fig. 7. The proposed antenna radiates an LHCP (RHCP) field when *Port* 1 (*Port* 2) is excited. The measured half power bandwidths (HPBW) are about 60° in both XZ and YZ planes, for both ports. The antenna performance of *Port* 1 and *Port* 2 are similar because of their symmetric structure. As shown in Fig. 8, the realized gains are larger than 7.2 dBic in the WLAN band, for both ports. The simulated radiation efficiency at each port is about −1 dB.

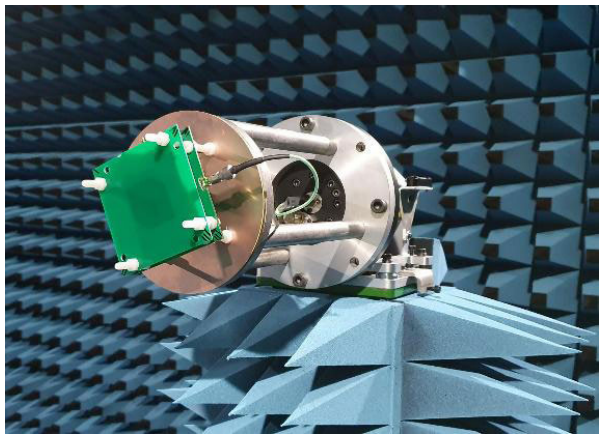

FIGURE 6. The antenna prototype in the anechoic chamber during radiation pattern measurements.

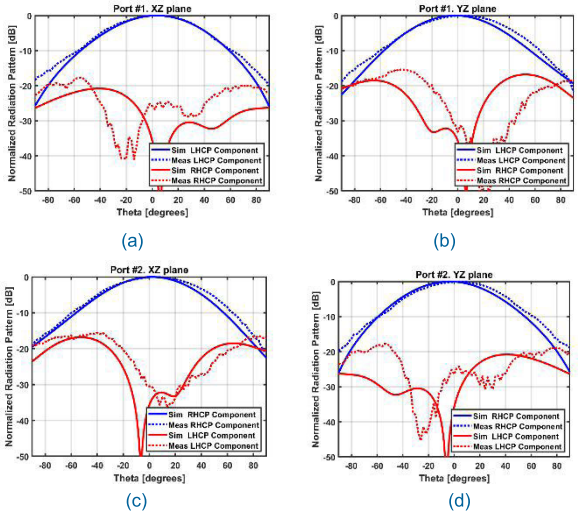

FIGURE 7. Simulated and measured normalized radiation patterns at 2.44 GHz (co-polar and cross-polar component): (a) XZ and (b) YZ planes,, when *Port* 1 is fed, and *Port* 2 is matched; (c) XZ and (d) YZ planes, when *Port* 2 is fed, and *Port* 1 is matched.

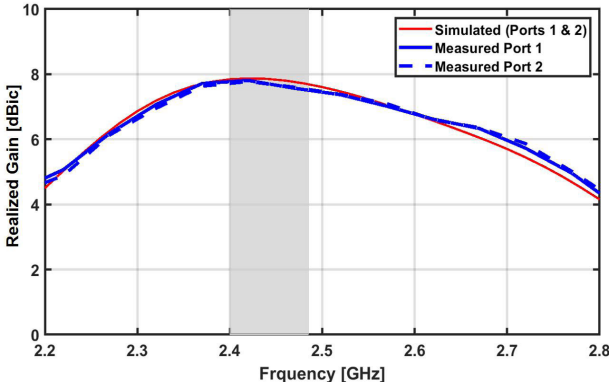

FIGURE 8. Realized gain in *Port* 1 mode or *Port* 2 mode.

The Axial Ratio (AR) at the broadside direction has been measured in the 2.2 - 2.8 GHz band, with a 50 MHz frequency step. Fig. 9 shows the simulated and measured AR of *Port* 1

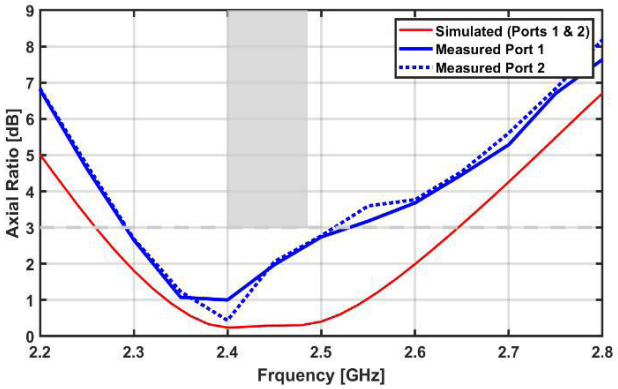

FIGURE 9. Simulated and measured axial ratio when *Port* 1 is fed or *Port* 2 is fed.

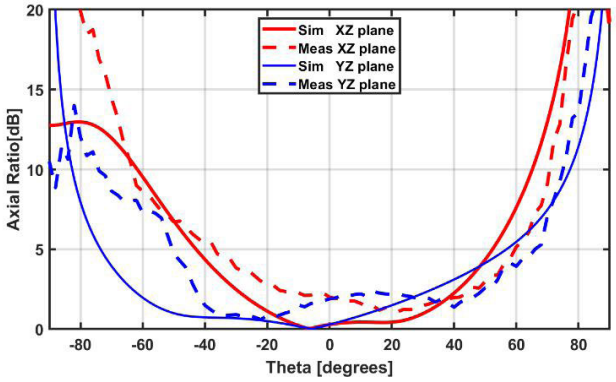

FIGURE 10. Simulated and measured axial ratio as a function of θ angle from broadside, in the XZ and YZ planes when *Port* 1 is fed, and *Port* 2 is matched.

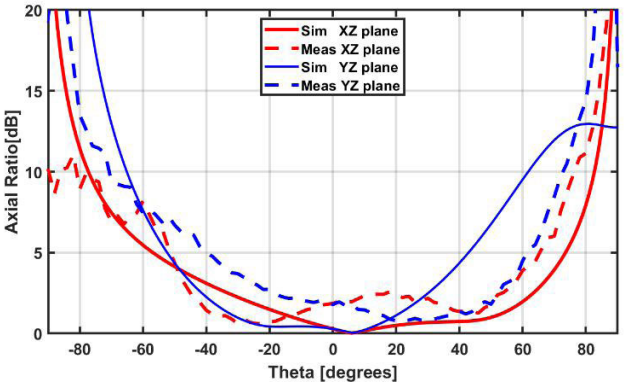

FIGURE 11. Simulated and measured axial ratio as a function of θ angle from broadside, in the XZ and YZ planes when *Port* 2 is fed, and *Port* 1 is matched.

and *Port* 2, respectively, exhibiting a reasonable agreement. In the simulation results, outstanding AR performance (under 3 dB) has been obtained from 2.25 to 2.65 GHz; it is less than 0.5dB in the −10dB impedance bandwidth. The AR measurement curve exhibits a slight rise at 2.5GHz when compared with the simulation curve. The possible reason is that the fabricated reflector with nylon fixed screws is not flat enough. In the testing process, the antenna to be measured could not be perfectly fixed over against the test antenna so that it would lead to axial ratio deterioration. The results of both the measured and the simulated AR variation versus the θ-angle at 2.44 GHz are shown in Fig. 10 and Fig. 11, respectively, for both ports. The AR in the XZ and YZ planes is below 3 dB in a beam of at least 60° around the broadside direction.

IV. A 4 × 4 MIMO WLAN ANTENNA SYSTEM

Two identical antennas are then used in a 4×4 MIMO WLAN configuration, and its performance has been estimated in terms of ECC and Channel Capacity, by considering a rich isotropic multipath (RIMP) scenario and a Rayleigh channel. By adding a second radiating element at a distance D, both polarization diversity and spatial diversity can be exploited at once. A 180-degree-rotation of the second element with respect to the first one is introduced to avoid overlapping of their feeding lines. Hence, all four ports are placed at the border of the structure, allowing for a simple connectorization with SMA connectors. The two-elements configuration which dimension is 157 mm × 96 mm × 39 mm is shown in Fig. 12.

The inter-element distance (D) is an important parameter to be set. A close spacing allows for a compact antenna size at the expense of a lower isolation, the latter increasing the signal correlation and making more difficult to achieve a satisfactory impedance matching at the receiver/transmitter sides [26]. As discussed in [26], the elements of the field transmission matrix become strongly correlated as the spacing between antennas drops below λ/4, if assuming that the significant rays are widely distributed in angle at the antenna array.

The two-antenna layout depicted in Fig. 12 has been numerically simulated. S-Parameters have been initially evaluated as a function of the inter-element distance, demonstrating good performance in terms of impedance matching ($S_{11} < -10$ dB) and mutual coupling ($S_{12} < -10$ dB) for distances D greater than 0.35 λ. Then, the six ECC curves have been calculated on the basis of the simulated radiation patterns [4], for different distances D. When the distance is greater than 0.35 λ, ECCs are lower than 0.5, which is usually an acceptable value for MIMO systems [28]–[30]. Multiplexing efficiency has been also evaluated as a function of the distance D. In [27] it has been defined as

$$\eta_{mux} = \frac{\rho_0}{\rho_T} \leq 1$$

which measures the loss of efficiency in SNR (or power, assuming the noise power σ_n^2 is the same) when using a real multiple-antenna prototype in an independent and identically distributed (i.i.d.) channel (with SNR ρ_T) to achieve the same capacity as that of an ideal array in the same i.i.d. channel (with SNR ρ_0). Multiplexing efficiency is a power-related metric for the spatial multiplexing mode of operation in MIMO systems. As it can be seen in Fig. 13,

TABLE 2. Performance comparison with other proposed CP MIMO system.

Ref.	Dimensions (λ is the wavelength at the central frequency of the -10dB-band)	Number of Ports	Multi Band	$B_{\%}$ (S_{11}<-10 dB) / Center Frequency	ARBW (<3dB)	Isolation (dB)	ECC	Gain @ Boresight(dBic)
[11]	0.24λ×0.24λ×0.01λ	2	Single band	5.7% / 2.45 GHz	4.1%	>17	<0.100	n.a.
[12]*	0.90λ×0.62λ×0.01λ	2	Triple-Band	18.8% / 3.51 GHz	5%	>18	<0.020	<3
[13]	0.18λ×0.18λ×0.01λ	2	Dual Band	36% / 2.625 GHz	32.6%	>18	<0.001	<2
[14]	0.55λ×0.55λ×0.20λ	2	Single Band	10.4% / 2.375 GHz	7.71%	>15	<0.003	<1.56
[15]	1.2λ×1λ×0.15λ	2	Single Band	10.28% / 5.155 GHz	4.17%	>14	<0.02	<5
This work	0.78λ×0.78λ×0.128λ	2	Single Band	7% / 2.425 GHz	8.1%	>25	<0.004	<8

* the radiating elements radiate two orthogonal LP fields at the WLAN band and two orthogonal CP fields in the range 3.31-3.48 GHz (within the WiMAX band). Antenna performance here indicated refers to the WiMAX band where a CP MIMO system is obtained.

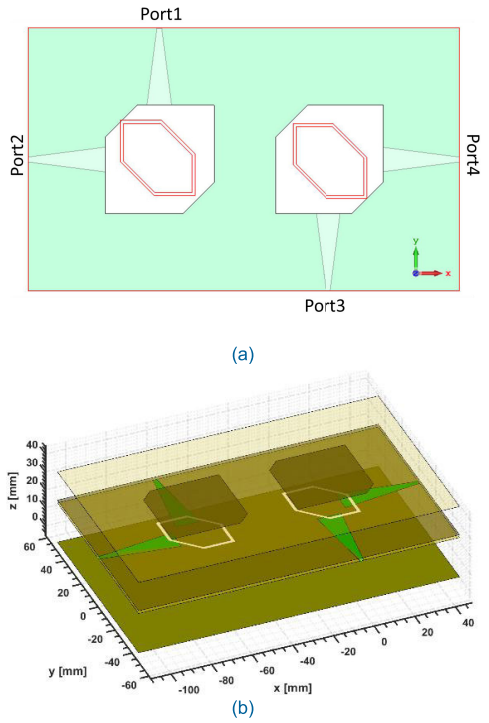

FIGURE 12. 2 × 2 MIMO configuration layout using two antennas with $D = 62$ mm spatial separation: (a) top view and (b) 3D view.

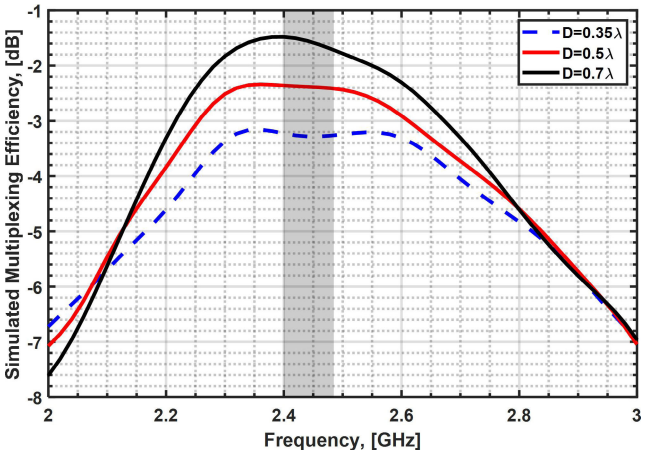

FIGURE 13. Simulated multiplexing efficiency as a function of the distance *D* between the two radiating elements.

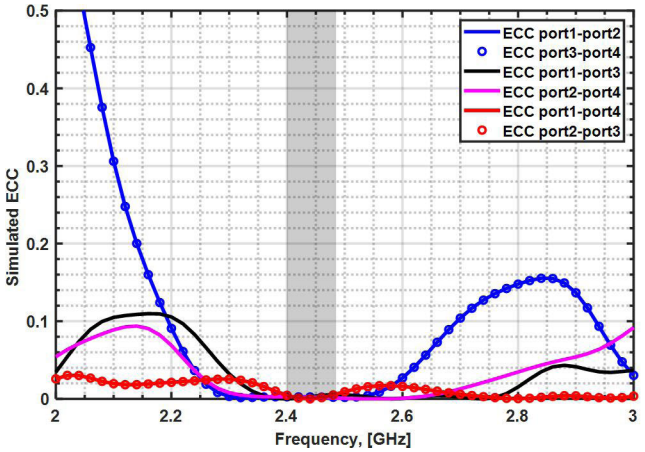

FIGURE 14. Simulated envelope correlation coefficient.

multiplexing efficiency decreases by reducing the inter-element distance D, and it results to be lower than -3 dB when $D = 0.35$ λ. An ECC lower than 0.5 and a multiplexing efficiency higher than -3dB are rules of thumb for designing MIMO systems [28]–[30].

As a trade-off between high isolation, low ECC, high multiplexing efficiency and antenna compactness, the two slot-coupled antennas are placed at a distance of 62 mm (∼0.5 λ). For such a configuration, all six ECCs assume values lower than 0.02 in the entire operating frequency band, as shown in Fig. 14.

Moreover, the channel capacity of a 4 × 4 MIMO scheme with spatial and polarization diversity can also be analyzed. Channel capacity is a system-level metric which expresses how many bits can be transmitted by exploiting 1 Hz of bandwidth. Thanks to the presence of four ports, it is possible to analyze the spatial diversity considering the two ports with the same polarization at each antenna, as well the spatial-polarization diversity considering ports with different

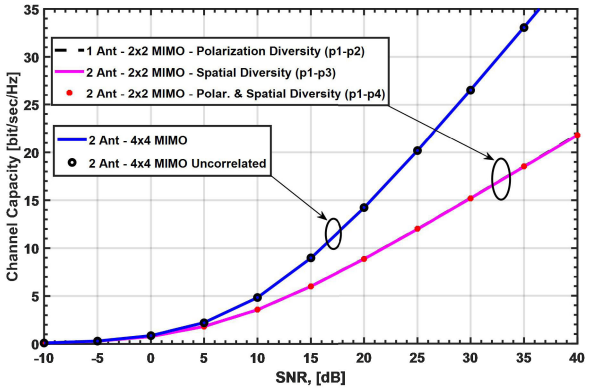

FIGURE 15. Channel capacity as function of the signal-to-noise ratio (SNR).

polarization at each antenna. In Fig. 15 the channel capacity for all above mentioned configurations is computed according to [27] and plotted as a function of the signal-to- noise ratio (SNR). It is shown that thanks to low values of ECC (lower than 0.01 in these considered scenarios), similar channel capacities are obtained in all the 2×2 MIMO schemes, for both spatial and polarization diversity. That means that the single patch antenna can be used for MIMO purposes using the polarization diversity of both ports. Also, the channel capacity significantly increases if the two equal antennas are used in a 4×4 MIMO scheme with both spatial and polarization diversity, as shown in Fig. 15. Since the six ECCs of the 4×4 MIMO antenna are lower than 0.01 (Fig. 14), the achieved channel capacity is comparable with that obtainable with uncorrelated fields (ECC = 0). The proposed dual-port dual-polarization antenna prototype allows for implementing a 4×4 MIMO configuration in a compact space. Compared with other CP WLAN antennas [11]–[15], the antenna presented in this paper may achieve both good isolation (>25 dB) and high gain (7 dBic), and results to be a good candidate for MIMO WLAN systems.

As shown in Table 2, the size and performance of the antenna are reported and compared with other already proposed solutions of antennas for CP MIMO WLAN systems. The proposed antenna in this paper achieves better isolation (>25 dB) as well as realized gain (7 dBic) and results to be a good candidate for MIMO WLAN systems.

V. CONCLUSION

A compact, two-port dual-circularly polarized MIMO antenna for WLAN applications has been designed, prototyped and characterized. Prototype measurements in terms of S-Parameters, axial ratio, radiation pattern and realized gain are in a good agreement with simulation results. Tapered-width stubs and different-width slot structure have been adopted to enhance the isolation and enlarge the impedance matching bandwidth. The antenna may be used in a 2×2 and a 4×4 MIMO system. Simulated performance in terms of envelope correlation coefficient and channel capacity demonstrates that the proposed layout is a good candidate for a CP MIMO WLAN system.

REFERENCES

[1] M. Agiwal, A. Roy, and N. Saxena, "Next generation 5G wireless networks: A comprehensive survey," *IEEE Commun. Surveys Tuts.*, vol. 18, no. 3, pp. 1617–1655, 3rd Quart., 2016.

[2] S. Sanayei and A. Nosratinia, "Antenna selection in MIMO systems," *IEEE Commun. Mag.*, vol. 42, no. 10, pp. 68–73, Oct. 2004.

[3] M. A. Jensen and J. W. Wallace, "A review of antennas and propagation for MIMO wireless communications," *IEEE Trans. Antennas Propag.*, vol. 52, no. 11, pp. 2810–2824, Nov. 2004.

[4] M. S. Sharawi, "Current misuses and future prospects for printed multiple-input, multiple-output antenna systems [wireless corner]," *IEEE Antennas Propag. Mag.*, vol. 59, no. 2, pp. 162–170, Apr. 2017.

[5] W. Jiang, L. Yang, B. Wang, and S. Gong, "A high isolation dual-band MIMO antenna for WLAN application," in *Proc. Int. Symp. Antennas Propag. (ISAP)*, Phuket, Thailand, Oct. 2017, pp. 1–2.

[6] J. R. Walton, M. S. Wallace, J. W. Ketchum, and S. J. Howard, "MIMO WLAN system," U.S. Patent 8 462 643 B2, Jun. 11, 2013.

[7] S. P. Biswal and S. Das, "Two-element printed PIFA-MIMO antenna system for WiMAX and WLAN applications," *IET Microw., Antennas Propag.*, vol. 12, no. 14, pp. 2262–2270, Nov. 2018.

[8] J. Deng, J. Li, L. Zhao, and L. Guo, "A dual-band inverted-F MIMO antenna with enhanced isolation for WLAN applications," *IEEE Antennas Wireless Propag. Lett.*, vol. 16, pp. 2270–2273, 2017.

[9] Q. L. Li, S. W. Cheung, D. Wu, and T. I. Yuk, "Optically transparent dual-band MIMO antenna using micro-metal mesh conductive film for WLAN system," *IEEE Antennas Wireless Propag. Lett.*, vol. 16, pp. 920–923, 2017.

[10] F. A. Dicandia, S. Genovesi, and A. Monorchio, "Analysis of the performance enhancement of MIMO systems employing circular polarization," *IEEE Trans. Antennas Propag.*, vol. 65, no. 9, pp. 4824–4835, Sep. 2017.

[11] L. Qu, H. Piao, Y. Qu, H.-H. Kim, and H. Kim, "Circularly polarised MIMO ground radiation antennas for wearable devices," *Electron. Lett.*, vol. 54, no. 4, pp. 189–190, Feb. 2018.

[12] N. K. Sahu, G. Das, A. Sharma, and R. K. Gangwar, "Design of a dual-polarized triple-band hybrid MIMO antenna for WLAN/WiMAX applications," in *Proc. IEEE Conf. Antenna Meas. Appl. (CAMA)*, Tsukuba, Japan, Dec. 2017, pp. 246–248.

[13] A. H. Haghparast and G. Dadashzadeh, "A dual band polygon shaped CPW-fed planar monopole antenna with circular polarization and isolation enhancement for MIMO aplications," in *Proc. 9th Eur. Conf. Antennas Propag. (EuCAP)*, Lisbon, Portugal, Apr. 2015, pp. 1–4.

[14] W. Li, K. W. Leung, and N. Yang, "Omnidirectional dielectric resonator antenna with a planar feed for circular polarization diversity design," *IEEE Trans. Antennas Propag.*, vol. 66, no. 3, pp. 1189–1197, Mar. 2018.

[15] N. K. Sahu, R. K. Gangwar, and P. Kumari, "Dielectric resonator based circularly polarized MIMO antenna for WLAN applications," in *Proc. 3rd Int. Conf. Microw. Photon. (ICMAP)*, Dhanbad, India, Feb. 2018, pp. 1–2.

[16] Y. Yao, X. Wang, X. Chen, J. Yu, and S. Liu, "Novel diversity/MIMO PIFA antenna with broadband circular polarization for multimode satellite navigation," *IEEE Antennas Wireless Propag. Lett.*, vol. 11, pp. 65–68, 2012.

[17] A. A. Pramudita, Sholihin, and D. D. Arianandа, "Array of eight circularly polarized microstrip antennas for IEEE 802.11ac MIMO WLAN," in *Proc. 4th Int. Conf. Sci. Technol. (ICST)*, Yogyakarta, Indonesia, Aug. 2018, pp. 1–6.

[18] J. Ha, M. A. Elmansouri, P. Valale Prasannakumar, and D. S. Filipovic, "Monostatic co-polarized full-duplex antenna with left- or right-hand circular polarization," *IEEE Trans. Antennas Propag.*, vol. 65, no. 10, pp. 5103–5111, Oct. 2017.

[19] R. Caso, A. A. Serra, M. Pino, P. Nepa, and G. Manara, "A wideband slot-coupled stacked-patch array for wireless communications," *IEEE Antennas Wireless Propag. Lett.*, vol. 9, pp. 986–989, 2010.

[20] R. Caso, A. Serra, A. Buffi, M. Rodriguez-Pino, P. Nepa, and G. Manara, "Dual-polarised slot-coupled patch antenna excited by a square ring slot," *IET Microw., Antennas Propag.*, vol. 5, no. 5, pp. 605–610, 2011.

[21] R. Caso, A. Buffi, M. Rodriguez Pino, P. Nepa, and G. Manara, "A novel dual-feed slot-coupling feeding technique for circularly polarized patch arrays," *IEEE Antennas Wireless Propag. Lett.*, vol. 9, pp. 183–186, 2010.

[22] A. Buffi, R. Caso, M. R. Pino, P. Nepa, and G. Manara, "Single-feed circularly polarised aperture-coupled square ring slot microstrip antenna," *Electron. Lett.*, vol. 46, no. 4, pp. 268–269, Feb. 2010.

[23] A. R. Guraliuc, A. Buffi, R. Caso, and P. Nepa, "Axial ratio analysis of single-feed circularly polarized resonant antennas," *J. Electromagn. Waves Appl.*, vol. 28, no. 6, pp. 716–728, Apr. 2014.
[24] D. M. Pozar, "Microstrip antenna aperture-coupled to a microstripline," *Electron. Lett.*, vol. 21, no. 2, pp. 49–50, Jan. 1985.
[25] R. Garg, P. Bhartia, I. J. Bahl, and A. Ittipiboon, *Microstrip Antenna Design Handbook*. Boston, MA, USA: Artech House, 2001, ch. 9.
[26] G. J. Foschini and M. J. Gans, "On limits of wireless communications in a fading environment when using multiple antennas," *Wireless Pers. Commun.*, vol. 6, no. 3, pp. 311–335, Mar. 1998.
[27] R. Tian, B. K. Lau, and Z. Ying, "Multiplexing efficiency of MIMO antennas," *IEEE Antennas Wireless Propag. Lett.*, vol. 10, pp. 183–186, 2011.
[28] W.-J. Liao, S.-H. Chang, J.-T. Yeh, and B.-R. Hsiao, "Compact dual-band WLAN diversity antennas on USB dongle platform," *IEEE Trans. Antennas Propag.*, vol. 62, no. 1, pp. 109–118, Jan. 2014.
[29] S. Nandi and A. Mohan, "A compact dual-band MIMO slot antenna for WLAN applications," *IEEE Antennas Wireless Propag. Lett.*, vol. 16, pp. 2457–2460, 2017.
[30] S. Zhang, A. A. Glazunov, Z. Ying, and S. He, "Reduction of the envelope correlation coefficient with improved total efficiency for mobile LTE MIMO antenna arrays: Mutual scattering mode," *IEEE Trans. Antennas Propag.*, vol. 61, no. 6, pp. 3280–3291, Jun. 2013.

ENZE ZHANG was born in Inner Mongolia, China, in 1992. He received the bachelor's and master's degrees in microwave engineering from the Harbin Institute of Technology, Harbin, China, in 2014 and 2016, respectively, where he is currently pursuing the Ph.D. degree.

From 2018 to 2019, he was a Visiting Scholar with the University of Pisa, Pisa, Italy. He focused on the research of dual-CP MIMO antenna for WLAN application. His current research interests include circularly polarized antennas, multi-band antennas, and microwave non-invasive glucose monitoring technology.

ANDREA MICHEL (Member, IEEE) received the B.E., M.E., (summa cum laude), and Ph.D. degrees in telecommunications engineering from the University of Pisa, Pisa, Italy, in 2009, 2011, and 2015, respectively.

He was a Visiting Scholar with the Electro Science Laboratory, The Ohio State University, Columbus, OH, USA, in 2014. He was involved in research on a theoretical analysis on the accuracy of a novel technique for deep tissue imaging. Since 2015, he has been a Postdoctoral Researcher in applied electromagnetism with the Microwave and Radiation Laboratory, Department of Information Engineering, University of Pisa, where he is currently an Assistant Professor. He is involved in the design of antennas for automotive applications, MIMO systems, and wearable communication systems, in collaboration with other research institutes and companies. His current research interests include design of integrated antenna for communication systems and smart antennas for near field UHF-RFID readers. He was a recipient of the Young Scientist Award from the International Union of Radio Science, Commission B, in 2014, 2015, and 2016, and the Best Paper Honorary Mention from the IEEE International Conference on RFID Technology and Applications, Shunde, Guangdong, China, in 2016. He serves as an Early Career Representative for URSI Commission B (Fields and Waves).

MARCOS RODRIGUEZ PINO was born in Vigo, Spain, in 1972. He received the M.Sc. and Ph.D. degrees in telecommunication engineering from the University of Vigo, Vigo, in 1997 and 2000, respectively. He was a Visiting Scholar with the Electro Science Laboratory, The Ohio State University, Columbus, OH, USA, in 1998. From 2000 to 2001, he was an Assistant Professor with the University of Vigo. Since 2001, he has been with the Electrical Engineering Department, University of Oviedo, Gijón, Spain, where he is currently an Associate Professor, teaching courses on communication systems and antenna design. He was a Visiting Fellow with the Department of Information Engineering, University of Pisa, Italy, in 2017, 2018 and 2019. His current research interests include antenna design, measurement techniques, and efficient computational techniques applied to EM problems, such as evaluation of radar cross section or scattering from rough surfaces.

PAOLO NEPA (Senior Member, IEEE) received the Laurea degree (summa cum laude) in electronics engineering from the University of Pisa, Pisa, Italy, in 1990.

Since 1990, he has been with the Department of Information Engineering, University of Pisa, where he is currently a Full Professor. He was a Visiting Scholar with the Electro Science Laboratory (ESL), The Ohio State University (OSU), Columbus, OH, USA, in 1998, where he was involved in efficient hybrid techniques for the analysis of large antenna arrays. In the context of UHF-RFID systems, he is working on techniques for radiolocalization of either tagged objects or readers. He has coauthored more than 300 international journal articles and conference papers. His current research interests include design of wideband and multiband antennas, and antennas optimized for near-field coupling and focusing. He is a member of the Technical Advisory Board of URSI Commission B—Fields and Waves. He was a recipient of the Young Scientist Award from the International Union of Radio Science, Commission B, in 1998. He served as the General Chair of the IEEE RFID-TA 2019 International Conference. Since 2016, he has been serving as an Associate Editor for the IEEE Antennas and Wireless Propagation Letters.

JINGHUI QIU was born in Heilongjiang, China, in 1960. He received the B.S. degree in radio engineering, the M.S. degree in communication and information systems, and the Ph.D. degree in communication and information systems from the Harbin Institute of Technology, in 1982, 1987, and 2008, respectively. From 1982 to 1987, he was a Teaching Assistant with the Harbin Institute of Technology. From 1987 to 1992, he was promoted as a Lecturer, and as an Associate Professor. He was promoted as a Professor, in 2002. He has authored or coauthored over 100 publications (book chapters, journal articles, and conference papers). His research interests include electromagnetic theory, microwave devices, antennas, and millimeter-wave imaging.